Control
and Cybernetics
VOL. 15 (1986) No. 3-4

Dynamic interactions in IRb robot

by

ANATOL GOSIEWSKI

WALDEMAR WIECZOREK

Institute of Automatic Control
Technical University of Warsaw
Nowowiejska 15/19
00-665 Warszawa, Poland

Results of simulation of dynamic interactions between the manipulator elements of IRb robot are presented in the paper. Particular attention is paid to the compensating influence of local servomechanisms action over these interactions. Interpretation of the results obtained and following conclusions may be significant in view of an application of IRb robots to CPC, as well as PTPC with reference trajectory of motion (e.g. time-optimal).

1. Introduction

IRb robot (as well as IRb 60) is equipped with three main servomechanisms controlling the motions of three main manipulator elements of that robot[1]. The system outputs of such a control system however, are not independent since they are interconnected by the dynamics of the plant i.e. the manipulator itself. We often define these interconnections as the dynamic interactions. For the process of PTPC type, when transfer trajectory from point to point in the operating space of a robot can be basically arbitrary, and no limitations occur apart from the natural ones (e.g. concerning some positions and admissible velocities) dynamic interactions do not play essential role and the control system described is generally sufficient. However in the case of the CPC or PTPC with given e.g. time-optimal trajectory, the problem is different and dynamic interactions may play essential role in view of the control implementation and accuracy.

The objective of this paper is presentation research results over the dynamic interactions in IRb-6 robot. The tests were carried out by the simulation technique on the computer MERA 400 in the Institute of Automatic Control of Warsaw

---

[1] Motion and control of the manipulator wrist is not involved in the subject and will not be considered.

Technical University within the research program over IRb robots (it can be expected that dynamic interactions in IRb-60 are qualitatively almost identical with the ones of IRb-6 since the robots differ only in the scale resulting from the value of parameters).

2. Manipulator dynamics and drives model

2.1. Exact model

The simplified kinematic scheme of IRB-6 robot manipulator is presented below. The manipulator is the system with three basic degrees of freedom and consists of rotating base (generalized coordinate — angle φ_1, lower link (coordinate φ_2) and upper link (coordinate φ_3) [5]. The manipulator elements are combined with each other by flat joints. The end of the upper link is connected by the joint with the manipulator wrist and the gripper (not indicated in Figure) having

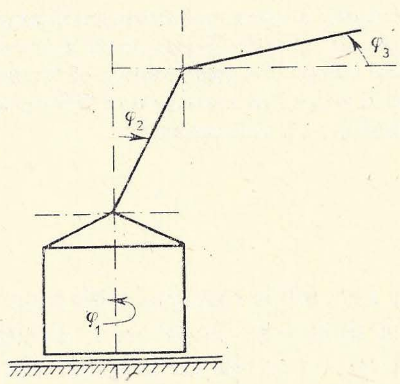

Simplified scheme of manipulator kinematics

two additional degrees of freedom. The self-dynamics of the wrist and gripper is negligible in comparison with the dynamics of basic manipulator elements and will not be analized here (apart from the punctual load of the upper link end). Each of the manipulator elements is driven by an individual d.c. motor over the gear: harmonic (column) and screw-spheric (links). Shafts rotation angles of individual motors are denoted ψ_1, ψ_2 and ψ_3 respectively.

The exact mathematical model of manipulator dynamics, taking into account operation and driving motors motion, has the form (see [5] and e.g. [4])

$$A(\boldsymbol{\varphi})\ddot{\boldsymbol{\varphi}}+B(\boldsymbol{\varphi},\dot{\boldsymbol{\varphi}})+C(\boldsymbol{\varphi})=Q(\boldsymbol{\varphi},\dot{\boldsymbol{\varphi}},t) \tag{1}$$

where

$\boldsymbol{\varphi}(t)=[\varphi_1(t)\ \varphi_2(t)\ \varphi_3(t)]^T \in R^3$ — coordinates vector

$\dot{\boldsymbol{\varphi}}(t)=[\dot{\varphi}_1(t)\ \dot{\varphi}_2(t)\ \dot{\varphi}_3(t)]^T \in R^3$ — velocities vector

$A(\varphi) \in R^{3\times 3}$ — matrix of system inertia, $A=A^T, A>0$
$B(\varphi, \dot{\varphi}) \in R^{3\times 1}$ — vector of torques of Coriolis's and viscous friction forces
$C(\varphi) \in R^{3\times 1}$ — vector of torques of gravitation forces
$Q(\varphi, \dot{\varphi}, t) \in R^{3\times 1}$ — vector of drive torques and dry friction forces.

Vector of driving torques M has the form

$$M=\left(\frac{\partial F}{\partial \varphi}\right)^T K I \tag{2}$$

whereas electrical dynamics model of motors is the equation

$$L I+R I+K \frac{\partial F}{\partial \varphi} \dot{\varphi}=E(t) \tag{3}$$

where

$F: R^3 \to R^3$ — function (nonlinear) relating coordinates vector φ with the rotation angles vector of motor shafts $\psi=[\psi_1\ \psi_2\ \psi_3]^T$: $\psi=F(\varphi)$
$I(t)=[I_1(t)\, I_2(t)\, I_3(t)]^T$ — vector of rotors currents
$F(t)=[E_1(t)\, E_2(t)\, E_3(t)]^T$ — vector of control voltages
$K=\text{diag}\,[K_1, K_2, K_3]$ — motors gain matrix
$R=\text{diag}\,[R_1, R_2, R_3]$ — resistance matrix of rotors
$L=\text{diag}\,[L_1, L_2, L_3]$ — inductance matrix of rotors.

The model defined by equations (1)–(3) is too complicated to be used directly for computer simulation and in consequence for investigating dynamic properties of the robot. An additional difficulty is that number of parameters occuring in that model is too big in relation to technical possibilities of their identification, not mentioning those parameters which are practically not identified at all. On the other hand, after initial assessments of masses values, centers of gravity, their inertia moments etc., it become clear that some elements of an accurate model can be ignored as they play no essential role in the research. In the result of analysis, such a simplification of the model proved to be both necessary and advisable which on one hand would preserve basic manipulator properties, and on the other allow for model's implementation in the computer simulation program of robot operation.

2.2. Simplified model

Most essential simplification of manipulator dynamics model concerns the description of its kinetic energy, hence the matrix $A(\varphi)$ [5]. Manipulator links are assumed to be stiff rods with inertia moments matrices (corresponding to non-inertial coordinates systems connected with the respective links) reduced to the form:

$$J_i=\begin{bmatrix} J_{11}^{(i)} & 0 & 0 \\ 0 & 0 & 0 \\ 0 & 0 & J_{33}^{(i)} \end{bmatrix}, \quad i=2, 3 \tag{4}$$

So this assumption means that only two main inertia moments of each link have non-zero values equal to each other ($J_{11}^{(i)}=J_{33}^{(i)}$). Inertia moment of the rotating base J_1 towards the axis of rotation is, of course, always a scalar quantity. Another simplification is ignoring a relatively slow rotation of the motor bulks suspended in a pendulous way on the rotating base.

In result of these simplifications four elements of the inertia matrix $A(\boldsymbol{\varphi})$, $A_{12}(\boldsymbol{\varphi})=A_{21}(\boldsymbol{\varphi})=A_{13}(\boldsymbol{\varphi})=A_{31}(\boldsymbol{\varphi})=0$, become equal to zero, while the remaining elements obtain a simpler form than previusly.

It has also proved true (which was to be expected) that the electric time-constant of driving motors are many times smaller than the characteristic time parameters of the manipulator i.e. that electrical dynamics (3) is many times faster than the manipulator dynamics (1). In a consequence motors were considered as non-intertial elements and rotors currents $I_1(t)$, $I_2(t)$ and $I_3(t)$ were assumed as control signals, which takes place in reality.

Expanding expressions for matrices $\boldsymbol{B}(\boldsymbol{\varphi}, \dot{\boldsymbol{\varphi}})$ and $C(\boldsymbol{\varphi})$ (see [5]) and taking into account (2) after simple transformations, having accepted simpliefied assumptions, we can now present the model of a system (1)–(3) in its "working" standard form of state equations in which the control vector becomes the vector of currents $\boldsymbol{I}(t)$

$$\dot{\boldsymbol{\varphi}}=\boldsymbol{\omega}$$
$$\dot{\boldsymbol{\omega}}=A^{-1}(\varphi)\left[-\frac{\partial U}{\partial \boldsymbol{\varphi}}-\operatorname{diag}\{b_i\}\,\boldsymbol{\omega}+\left(\frac{\partial F}{\partial \boldsymbol{\varphi}}\right)^T KI(t)-\right.$$
$$\left.+\left(\omega_1\frac{\partial A}{\partial \varphi_1}+\omega_2\frac{\partial A}{\partial \varphi_2}+\omega_3\frac{\partial A}{\partial \varphi_3}\right)\boldsymbol{\omega}+\begin{bmatrix}\boldsymbol{\omega}^T\frac{\partial A}{\partial \varphi_1}\boldsymbol{\omega}\\ \boldsymbol{\omega}^T\frac{\partial A}{\partial \varphi_2}\boldsymbol{\omega}\\ \boldsymbol{\omega}^T\frac{\partial A}{\partial \varphi_3}\boldsymbol{\omega}\end{bmatrix}\right] \qquad (5)$$

where

$\boldsymbol{\omega}(t)=[\omega_1(t)\,\omega_2(t)\,\omega_3(t)]^T$ — velocity vector,

$U(\boldsymbol{\varphi})$ — potencial energy of manipulator,

$\operatorname{diag}\{b_1, b_2, b_3\}$ — matrix of viscous friction coefficients.

We do not discuss here non-linear expressions for non-zero elements of matrix $A(\boldsymbol{\varphi})$, vector function $\boldsymbol{F}$ and potencial energy U as meaningless ones for further considerations.

Model (5) has been implemented into computer simulation program of IRb robot operation.

2.3. Structure of servomechanisms

Each element (degree of freedom) of manipulator is controlled by means of its own local servomechanism. The structure of control system is presented in Figure below.

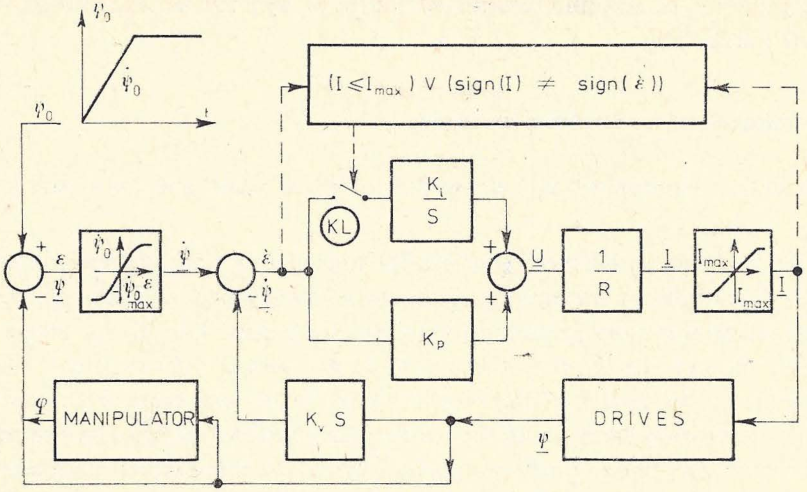

Manipulator control system

In servomechanisms two loops of negative feedback occur: through the resolver from the position of motor rotor (external loop) and through tachogenerator with the gain K_v from the retor speed (internal loop). The reference signal for the external loop is the signal $\psi_0(t)$, which for the task of displacement is determined by three quantities: initial position ψ_{0i}, final position ψ_{0f} and the rotor speed $\dot{\psi}_0=\dot{\varphi}_0 n_m$, where $\dot{\varphi}_0$ — given velocity of respective coordinate and n_m — mean gear ratio between the coordinate velocity and rotor speed $\left(d\psi=\frac{\partial F}{\partial \varphi}\, d\varphi\right)$. The reference signal $\dot{\psi}_0$ for internal loop i.e. for the speed controller *PI* is the position error signal on transmitting over the transducer having the square characteristic with saturation (approximated by three segments). Saturation value corresponds to the maximum reference velocity of displacing $\dot{\psi}_0$ max.

Controllers *PI* in IRb robots are realized in analogue technique, thus their range of linear operation is essentially and intentionally bounded by the field of voltages supplying operation amplifiers. That non-linearity of a real controller *PI* was included into the simulation program by means of the switch *KL* which switching on sets into operation the integrator K_J/s. The condition when the swith is "on" (linear operation) is determined by the alternative

$$(I \leqslant I_{\max}) \vee (\operatorname{sign} I \neq \operatorname{sign} \dot{\varepsilon}) \tag{6}$$

where $\dot{\varepsilon}=\dot{\psi}_0-\dot{\psi}$, I — control current, $I_{\max}$— current constraint When the alternative (6) assumes logical value 0, the switch is set to "off" position (enter on voltages field bound), the integration process interrupted, and on the output of an integrator its present state is stored.

3. The influence of servomechanisms operation on dynamic interactions in IRb robot manipulator

3.1. Characteristic of the simulation experiment

Simulation experiment was composed of three parts and each part of seven stages.

In the first part (I) the motion of manipulator elements and dynamic interactions between them **without** servomechanisms were investigated and the jumps (steps) of control currents were imparted to the motors inputs. During the stages 1–3 of this part, the current jump was imparted to the motor only of one manipulator element i.e. to the motor of the rotating base, lower and upper link successively while two remaining elements of the manipulator were not driven, having remained practically at the initial positions corresponding to mechanical constraints. The motion of the manipulator element driven in conditions like those we shall call an **isolated motion** (it plays a role of the reference motion). Within the stages 2–6, current jumps were imparted to the motors of two manipulator elements (base and lower link, base and upper link, lower link and upper link), while the third manipulator element remained at the initial position. Hence, stages 2–6 make possible to define the motion influence of each manipulator element over another one assuming isolated motion as a reference. Finally, during the stage 7, the current jumps were imparted to all three manipulator motors which made posible to define the influence of motion of each pair of elements over the third element, taking again the isolated motion as the basis of comparison. The values of current jumps were adjusted to be the same for the same motors at each experiment stage of part I.

The second part of the experiment (II) was analogical to part I, differed, however, by having tested the motion of manipulator elements and dynamic interactions between them **with** servomechanisms, at which the position reference signals were the signals of "ramp" type, described in section 2.3. Similarly to part I, successive stages (1–7) of part II made possible to estimate the interaction between respective manipulator elements and, by comparison with the respective stages of part I, to observe the compensative action of servomechanisms (for which each interaction may be considered as a specific disturbance of their operation).

3.2. Simulation experiment data

The basic servomechanisms and drives data: $K_p=10{,}0\ V/V$, $K=145{,}9\ V/V$, $K_v=0{,}028-0{,}046\ V\ \mathrm{rad}/s$, $\psi_{0\,\max}=12\ V$, $I_{\max}=11{,}0, A$, $R=R_{eq}=0{,}9$, max $\dot{\psi}=$ $=3000$ rev/min, $n_m=160{,}0$–$166{,}0$. Load of the upper link — maximal=6 KG. Data concerning manipulator parameters of IRb robot (non-essential for further analysis) can be found in operating instructions for IRb robot and in [5]. Data concerning variables are in the Table below.

STAGE	φ_{01i}	φ_{02i}	φ_{03i}	φ_{01f}	φ_{02f}	φ_{03f}	φ_{0j} $j=1, 2, 3$	I_1	I_2	I_3
I	0	40°	−40°	x	bound (−40°)	bound (25°)	x	4.0	−8.5	4,5
II	0	40°	−40°	60°	−35°	23°	90°/s	x	x	x

3.3. Simulation experiment results and their interpretation

Simulation results are presented in Fig. 1–6 in the form of diagrams of time-responses of respective coordinates $\varphi_j(t)$ and their velocities $\dot{\varphi}_j(t)$, $i=1, 2, 3$. Fig. 1, 3 and 5 correspond to the first part of the experiment, while Fig. 2, 4 and 6 — correspond to the second part, (such an arrangement of diagrams allows for more convenient comparison of manipulator elements behaviour **without** servomechanisms and **with** them). The isolated motion of a given element in each diagram is drawn

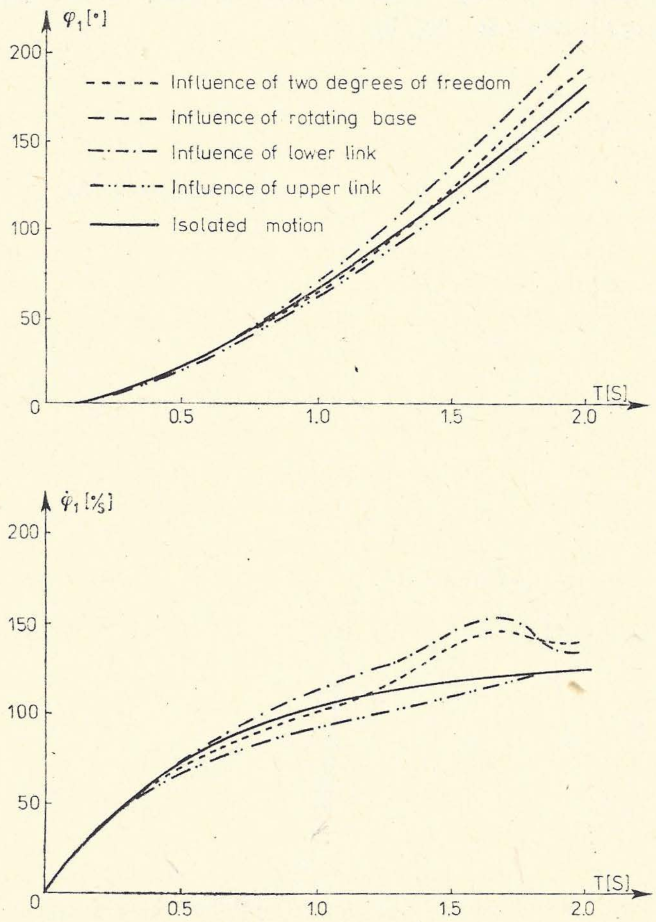

Fig. 1. Rotating base I

in continuous line and is the reference, on the other hand, the motion of this element with the influence of other elements motion is drawn in a respective dashed line (see description of Fig. 1).

The basic conclusions resulting from simulation experiment are as follows:

(i) The interaction character between manipulator elements with servomechanisms and without them and their physical interpretation is, on the whole, very similar.

(ii) Interactions between manipulator elements **with** servomechanisms are radically smaller than the same ones **without** servomechanisms which to a certain extent was to be expected.

(iii) The main cause of the interactions is centrifugal inertia force rising at the rotating base motion. The influence of changes of effective inertia moments is smaller than expected.

(iv) The influence of rotating base motion over the lower link motion (Fig. 3 and 4) is the strongest one. The reverse influence is many times smaller, particularly **with** servomechanisms (Fig. 2).

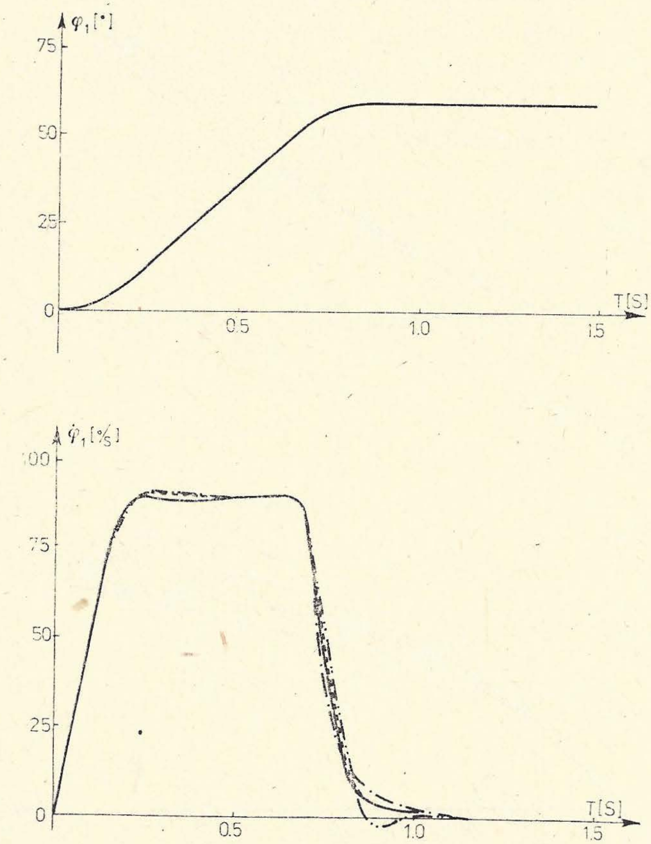

Fig. 2. Rotating base II

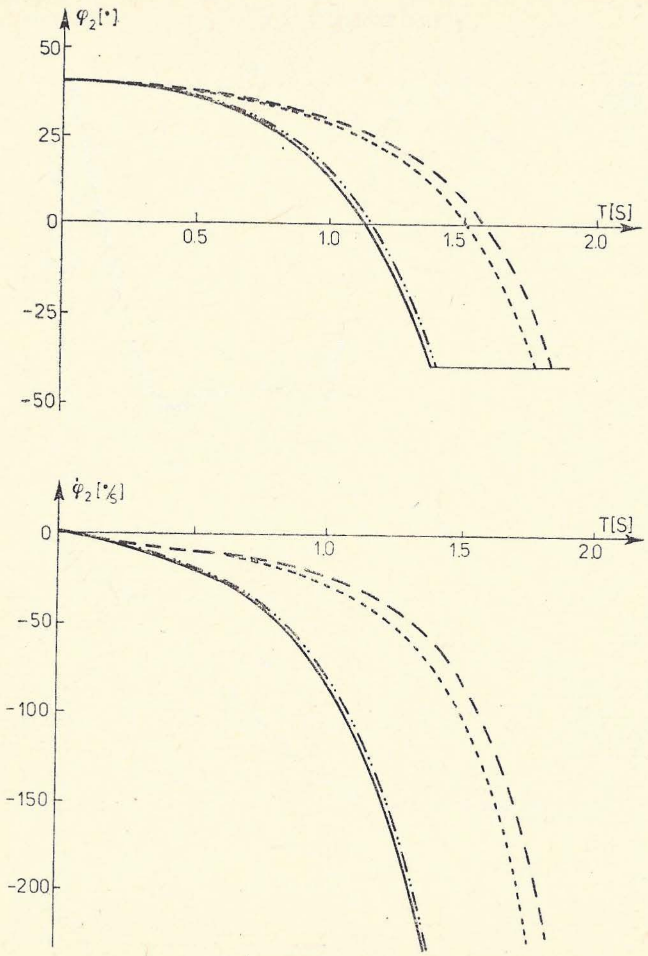

Fig. 3. Lower link I

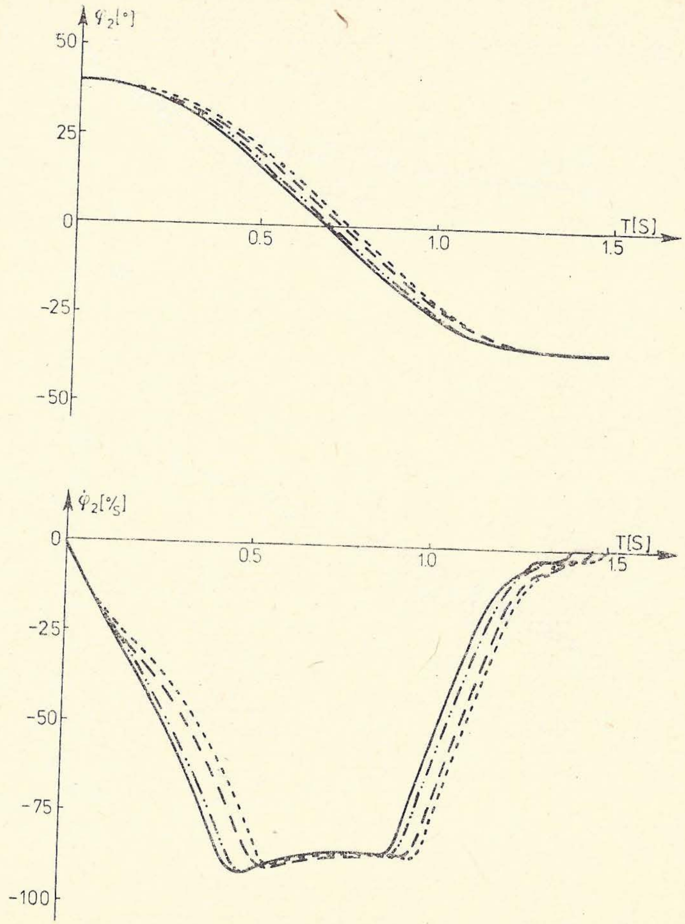

Fig. 4. Lower link II

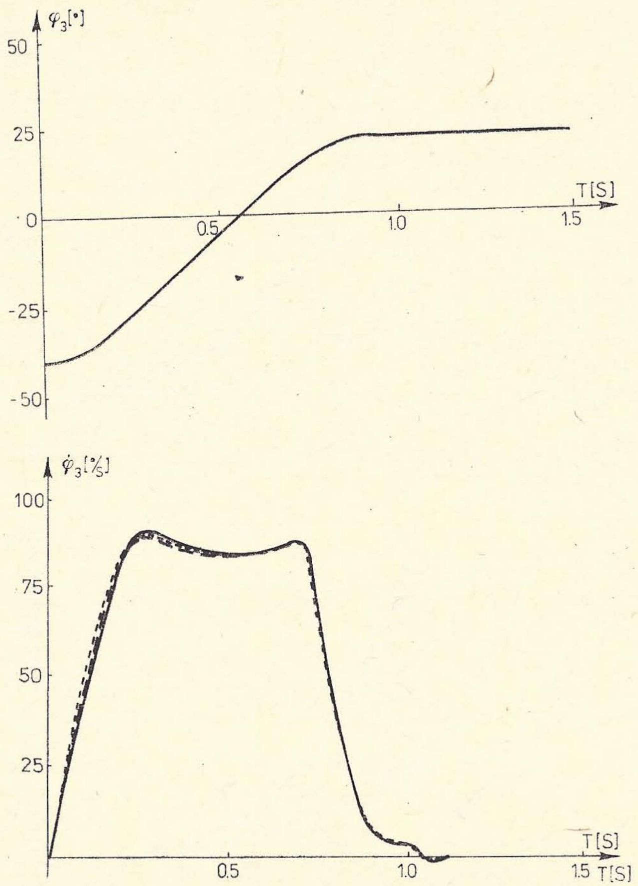

Fig. 5. Upper link I

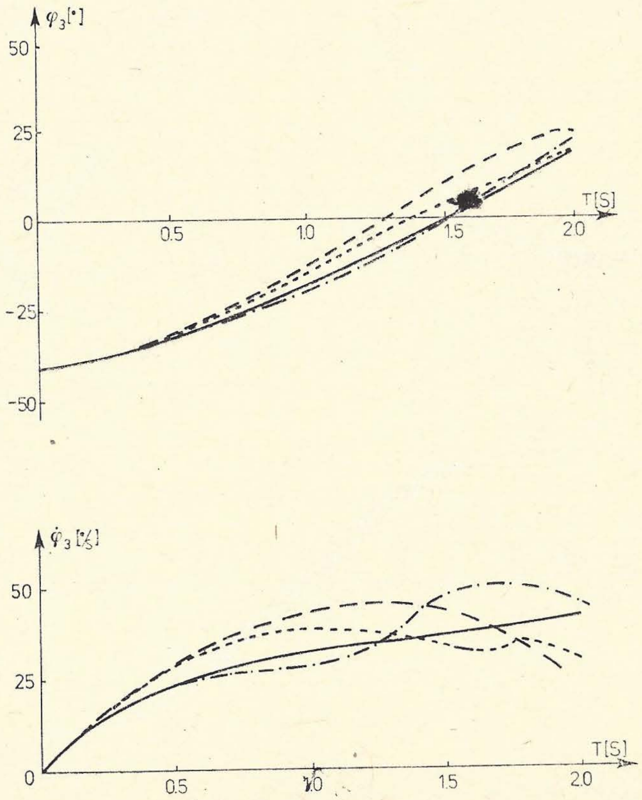

Fig. 6. Upper link II

(v) The influence of the upper link motion over the lower link motion with servomechanisms (Fig. 4) is of an importance too. It is, however, over twice smaller than the influence mentioned in (iv) (Fig. 6).

(vi) The influence of two manipulator elements (degrees of freedom) over the remaining one is in almost each case stronger than interactions between an arbitrary pair of elements.

(vii) All weak interactions in part II of the experiment (Fig. 2 and 6) are so small that can be only observed on the diagrams of velocity responses $\dot{\varphi}_1 (t)$; the differences in position responses $\dot{\varphi}_1 (t)$ are so small that the respective curves overlap with the curves of isolated motions.

Interactions between particular manipulator elements (degrees of freedom) with servomechanisms are presented in the Table below in which the values of coordinates deviations φ_i from trajectory of respective isolated motion were compared.

INFLUENCE \ EFFECT	Rotating base φ_1	Lower link φ_2	Upper link fφ_3
Rotating base	X	$<5°$	$<1°$
Lower link	$<1°$	X	$<1°$
Upper link	$<1°$	$<2°$	X
Two degrees of freedom	$<1°$	$<7°$	$<1°$

Some illustration of dynamic interactions influence between the manipulator elements over the accuracy of robots operation is the maximum magnitude deviation between trajectory which would be marked off by the end of the upper link (wrist with a gripper) in the operating Cartesian space at composing three isolated motions $\varphi_1 (t)$, $\varphi_2 (t)$, $\varphi_3 (t)$ and the most "disadvantageous" trajectory resulting from a simultaneous composing the motion of all three manipulator elements (the last row of interactions Table). As it was calculated, when displacing from point to point, this maximum deviation magnitude is about 55 mm which is a remarkable value.

4. Conclusions

The results presented above only partly show dynamic interactions in IRb Robot, as we have to take into account a very strong nonlinearity of analized system. Nevertheless the results quite distincly show that in general, the operation of this robot with the functioning control system, at the given trajectory in operating space e.g. at CPC, does not seem to be possible in use due to inaccuracy of reconstruction (perhaps apart from trajectories being in the plane pasing through the axis of rotation of the rotating base). Thus, these results suggest a necessity to use an upper level regulator with CPC, the one that would effectively compensate dynamic interactions in the system. Such an upper level regulator is often discussed in bibliography of the subject. Its structure is either based on various ideas of adaptation system with reference model (MRAC — see e.g. [1], [3]) or on the idea of decouplling and linearizing system [2]–[5].

References

[1] Balestrino A., De Maria G., Sciavice L. An Adaptation Model Following Control for Robotic Manipulators. *Transactions of the ASME*, **105** (1983).

[2] Banaszak Z., Jacak W. Controlling with a robot basing on the model of its dynamics, Papers from the X th Polish Conference Theory of Machines and Mechanisms. Warsaw, 1984.

[3] Dubowsky B., Des Forges D. T. The Application of Model-Referenced Adaptive Control to Robotic Manipulators. *Transactions of the ASME*, **101** (1979).

[4] Paul R. P. Robot Manipulators, The MIT Press, 1982.

[5] Research Report of the Institute of Automatic Control of Warsaw Technical University: Investigations over Dynamics of IRb-6 and IRb-60 Robots and Design of Tracking Control System, Project 06.6, PR-01.03.04, stage I, 1984.

Dynamika współzależności ruchu elementów robota IRb

W pracy przedstawiono wyniki symulacji dynamicznych współzależności ruchu elementów robota IRb. Szczególną uwagę zwrócono na kompensacyjny wpływ pracy lokalnych serwomechanizmów na te współzależności. Wyniki analizy otrzymanych rezultatów mogą być wykorzystane przy zastosowaniu robotów IRb do pracy w systemie CPC lub PTPC.

Динамика взаимозависимости движения элементов робота IRb

В работе представлены результаты моделирования динамических взаимозависимостей движения элементов работа IRb. Особое внимание обращено на компенсационное влияние работы локальных сервомеханизмов на эти взаимозависимости. Анализ полученных результатов может быть использован при применении работов IRb для работы в системе CPC или PTPC.